# A robust optical parametric oscillator and receiver telescope for differential absorption lidar of greenhouse gases

**Citation for published version:**
Robinson, I, Jack, J, Rae, C & Moncrieff, J 2015, A robust optical parametric oscillator and receiver telescope for differential absorption lidar of greenhouse gases. in *Proceedings of SPIE.* vol. 9645, 9645OU, SPIE, SPIE Remote Sensing 2015, Toulouse, United Kingdom, 21/09/15. https://doi.org/10.1117/12.2197251

**Digital Object Identifier (DOI):**
10.1117/12.2197251

**Link:**
Link to publication record in Edinburgh Research Explorer

**Document Version:**
Publisher's PDF, also known as Version of record

**Published In:**
Proceedings of SPIE

# A robust optical parametric oscillator and receiver telescope for differential absorption lidar of greenhouse gases

Iain Robinson[a], James W. Jack[a], Cameron F. Rae[b], John B. Moncrieff*[a]
[a]School of GeoSciences, University of Edinburgh, Crew Building, The King's Buildings, Alexander Crum Brown Road, Edinburgh, Scotland, UK. [b]Photonics Innovation Centre, School of Physics and Astronomy, University of St Andrews, North Haugh, St Andrews, Scotland, UK

## ABSTRACT

We report the development of a differential absorption lidar instrument (DIAL) designed and built specifically for the measurement of anthropogenic greenhouse gases in the atmosphere. The DIAL is integrated into a commercial astronomical telescope to provide high-quality receiver optics and enable automated scanning for three-dimensional lidar acquisition. The instrument is portable and can be set up within a few hours in the field.

The laser source is a pulsed optical parametric oscillator (OPO) which outputs light at a wavelength tunable near 1.6 μm. This wavelength region, which is also used in telecommunications devices, provides access to absorption lines in both carbon dioxide at 1573 nm and methane at 1646 nm. To achieve the critical temperature stability required for a laser-based field instrument the four-mirror OPO cavity is machined from a single aluminium block. A piezoactuator adjusts the cavity length to achieve resonance and this is maintained over temperature changes through the use of a feedback loop. The laser output is continuously monitored with pyroelectric detectors and a custom-built wavemeter.

The OPO is injection seeded by a temperature-stabilized distributed feedback laser diode (DFB-LD) with a wavelength locked to the absorption line centre (on-line) using a gas cell containing pure carbon dioxide. A second DFB-LD is tuned to a nearby wavelength (off-line) to provide the reference required for differential absorption measurements. A similar system has been designed and built to provide the injection seeding wavelengths for methane. The system integrates the DFB-LDs, drivers, locking electronics, gas cell and balanced photodetectors.

The results of test measurements of carbon dioxide are presented and the development of the system is discussed, including the adaptation required for the measurement of methane.

**Keywords:** DIAL, OPO, lidar, lasers, greenhouse gases, GHG

## 1. INTRODUCTION

Lidar is a key remote sensing technique for atmospheric monitoring [1] using pulses of laser light to study the structure and composition of the atmosphere. The differential absorption technique [2] is an enhancement which can probe specific atmospheric constituents by targeting their optical absorption lines. Differential absorption lidar (DIAL) has proven adept at identifying and quantifying trace gases and elements in the atmosphere. The key advantage of DIAL is that it enables the spatial distribution of an atmospheric constituent to be mapped out.

There is an acute need for methods which can monitor greenhouse gas emissions, both to compile and verify inventories and to aid in understanding the carbon cycle. The two most important anthropogenic greenhouse gases are carbon dioxide ($CO_2$) and methane ($CH_4$) and these have become the key targets for lidar measurement. DIAL has been used to quantify $CO_2$ emissions from industrial sources [3] and monitor leaks from carbon sequestration sites [4].

DIAL works by using a transmitter which fires a laser pulse into the atmosphere that is at an absorption wavelength (the *on-line* wavelength) of the target gas. The pulse is scattered in all directions from molecules and aerosols in the atmosphere. A tiny fraction of the scattered light is collected by a receiver telescope adjacent to, or co-aligned with, the transmitter. The laser wavelength is then re-tuned to a non-absorbing wavelength (the *off-line* wavelength) and another measurement made. By using the *off-line* measurement as a reference the concentration of the target gas can be calculated. Because the system is pulsed, the signal contains information about where the absorption occurs. This *range-resolved* feature of lidar, combined with the ability to mechanically scan the laser beam direction provides the spatial resolution in lidar measurements.

*J.Moncrieff@ed.ac.uk; phone +44 131 650 5402; http://www.geos.ed.ac.uk/~irobinso/lidar/

Lidar Technologies, Techniques, and Measurements for Atmospheric Remote Sensing XI,
edited by Upendra N. Singh, Doina Nicoleta Nicolae, Proc. of SPIE Vol. 9645, 96450U
 · doi: 10.1117/12.2197251

The requirements for a greenhouse gas DIAL are demanding. As only a tiny fraction of the transmitted pulse energy is collected by the receiver telescope the laser pulse energy must be high, but still within eye-safety limits [5]. The spectrally-narrow absorption lines in $CO_2$ (39 pm full width at half maximum) and $CH_4$ (35 pm) mean that the laser must have a spectral width substantially narrower than the absorption lines being targeted. The *on-line* wavelength must be precisely and accurately tuned into the centre of the absorption line, yet must also be capable of rapidly retuning to the *off-line* wavelength on a timescale much faster than changes in the atmosphere. The beam quality must be good enough to transmit a low-divergence beam that can travel many kilometres. Finally, the receiver aperture must have a large diameter to collect as much of the scattered light as possible and a high-sensitivity detector to record it.

This combination of demanding requirements means that DIAL systems are often bulky with high power consumption, making them challenging to use in the field. The design goals for this instrument are that it must be portable, reliable and capable of assembly and operation by two people in the field. There are a number of choices of wavelength region for DIAL systems, including $CO_2$ systems at 1.6 μm [3,6] and 2 μm [7]. We choose the 1.6 μm region because a profusion of telecommunications devices, particularly high-sensitivity detectors [8], operate in this wavelength region. It also provides access to $CH_4$ absorption lines [9].

In this article we will describe the instrument we are developing and how it addresses the requirements both for meeting the exacting demands for DIAL of greenhouse gases and maintaining the system as a portable practical field instrument within these constraints.

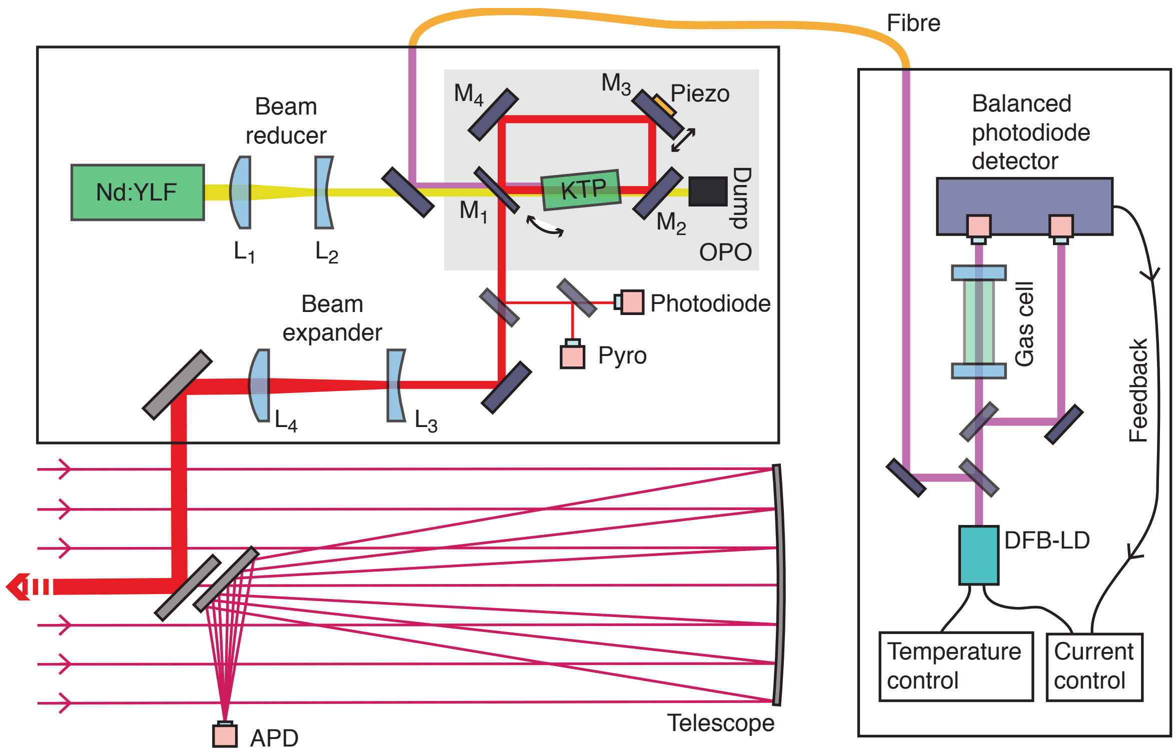


Figure 1: diagram of a differential absorption lidar for measurement of greenhouse gases. A pulsed diode-pumped neodymium-doped yttrium lithium fluoride (Nd:YLF) laser is reduced in diameter by a pair of lenses ($L_1$ and $L_2$) and pumps a four-mirror ($M_1$, $M_2$, $M_3$ and $M_4$) optical parametric oscillator (OPO) with a potassium titanyl phosphate (KTP) non-linear crystal. The cavity is injection-seeded by a continuous-wave distributed feedback laser diode (DFB-LD). The beam is expanded by a pair of lenses ($L_3$ and $L_4$) and fired into the atmosphere. The returning signal is collected by the telescope, detected with an avalanche photodiode (APD), and then digitized with a fast analogue-to-digital converter.

Figure 2: The laser system mounted on the telescope. A diagram of the system is shown in Figure 1.

## 2. INSTRUMENT OVERVIEW

Figure 1 is a diagram of the instrument showing the two main components: a receiver telescope to which the laser transmitter attaches directly, and an injection-seeding system. A photograph of the laser mounted on the telescope is shown in Figure 2.

A neodymium-doped yttrium lithium fluoride (Nd:YLF) laser is pumped by a pulsed laser diode with a wavelength of 808 nm though an optical fibre (not shown in the diagram). The Nd:YLF laser is Q-switched and outputs pulses at 1047 nm wavelength, 50 Hz pulse repetition frequency, and 4.6 mJ energy per pulse. The output beam diameter is reduced by a pair of lenses ($L_1$ and $L_2$ in Figure 1) to increase the radiant exposure of the beam entering the optical parametric oscillator (OPO).

The OPO is a four-mirror ($M_1$, $M_2$, $M_3$ and $M_4$ in Figure 1) cavity surrounding a potassium titanyl phosphate (KTP) non-linear crystal. KTP has been used in a number of OPO systems for spectroscopic applications [10, 11]. The OPO converts the Nd:YLF wavelength (1047 nm) to a signal wave around 1600 nm and an idler wave around 3000 nm. The residual (Nd:YLF) pump makes a single pass through the non-linear crystal and leaves the cavity, along with the idler wave, through $M_2$. The cavity is resonant only at the signal wavelength (1600 nm) and this is the only wavelength used for lidar measurements. To ensure the OPO is both mechanically stable and temperature stable it is manufactured from a single aluminium block, shown in Figure 3. The non-linear crystal is mounted in a rotatable mount to (coarsely) tune the signal wavelength.

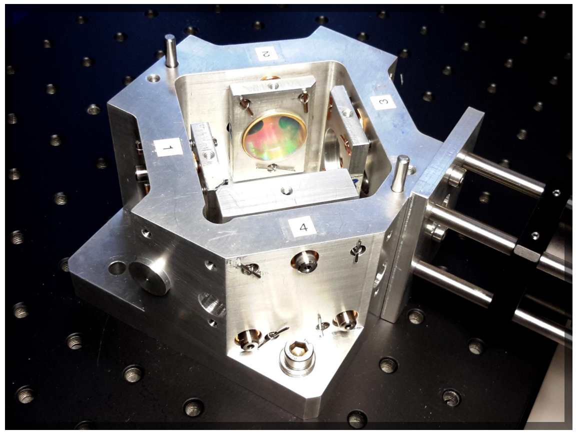

Figure 3: the optical parametric oscillator (OPO) is machined from a single aluminium block to maximise temperature stability and mechanical rigidity.

For fine tuning of the signal wavelength, and to ensure it is in the centre of the absorption line of the target greenhouse gas, the OPO cavity is injection-seeded with a continuous-wave distributed feedback laser diode (DFB-LD in Figure 1). The DFB-LD is fired into the OPO on the same path as the (Nd:YLF) pump. It is tuned to the absorption line of the target gas ($CO_2$ or $CH_4$) by measuring the absorption in a gas cell using a custom-designed balanced photodiode pair. Injection seeding the OPO enables operation at a precisely-defined wavelength and narrows the spectral width of the output [12].

To ensure the cavity is on resonance at the *on-line* (or *off-line*) wavelength the cavity length is fine-tuned with a piezoelectric actuator attached to $M_3$ (Piezo in Figure 1). A fraction of the output light from the cavity is picked off into a photodiode while the cavity length is scanned by ramping the voltage on the piezo from 0 to 100 V. When the cavity comes onto resonance the output exhibits a pronounced dip. This *intensity dip signal* [12] is measured by the photodiode and fed back to the piezo using a dither-and-lock technique. This ensures that the cavity is always on resonance at the injection seeded wavelength. (The feedback loop is momentarily frozen at the moment the Nd:YLF pump pulse is fired.)

Two similar interchangeable injection seed sources were developed for use with the instrument for $CO_2$ (Figure 4A) and $CH_4$ (Figure 4B). The $CO_2$ system uses a DFB-LD tuned to the absorption line at 1572.992 nm [13]. A multipass Heriott-type absorption cell with a 36 m path length is used to detect the relatively-weak absorption in a sample of pure $CO_2$. In contast, the methane absorption lines around 1645.552 nm [8] are 74 times stronger allowing a short (0.1 m) gas cell to be used. The seed sources units for $CO_2$ and $CH_4$ are shown in Figure 4. The output of the seed source is fed to the OPO on an optical fibre (Figure 1).

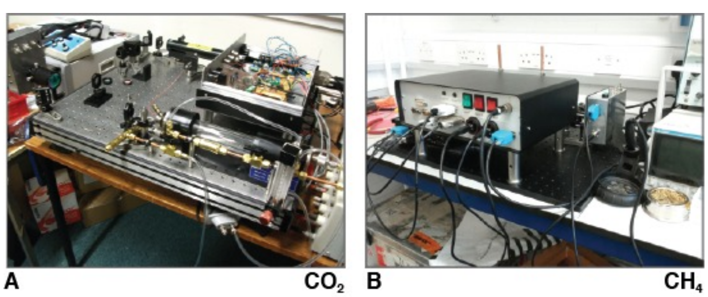


Figure 4: the interchangeable carbon dioxide (**A**) and methane (**B**) injection seed sources.

## 3. RESULTS AND DISCUSSION

Figure 5 shows absorption measurements of $CO_2$ and $CH_4$ made with the corresponding seed units. The measurements are compared to calculations of the transmittance of the atmosphere over a 1 km path length. These calculations were made using data from the HITRAN2012 database [14]. The transmittance spectra of pure $CO_2$ (Figure 5C) and pure $CH_4$ (Figure 5D) were also measured in their respective gas cells. The widths of the lines measured in the gas cells are broader than the atmospheric calculations due to pressure broadening. Finally, the absorbance of the DFB-LD by $CO_2$ in the atmosphere was measured over a 100 m (open) path length. The $CO_2$ signal (Figure 5E) has a varying background and this is likely due to variations in the laser intensity during the measurement. The use of the balanced photodiode detector should eliminate this problem. There is also a small offset in the line positions between the measurement and the calculation which is likely to be a wavelength calibration error.

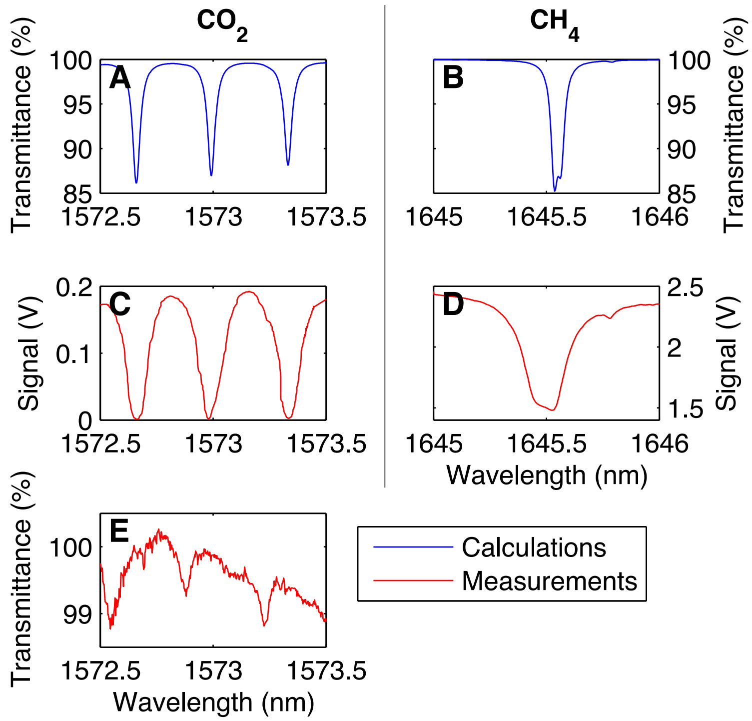


Figure 5: The calculated atmospheric transmittance spectra for $CO_2$ (**A**) and $CH_4$ (**B**) over a 1 km path length. The transmittance spectrum of pure $CO_2$ was measured in a 36 m long gas cell (**C**) and pure $CH_4$ in a 0.1 m long gas cell (**D**). The transmittance spectrum of the atmosphere was measured over a 100 m path length (**E**).

Figure 6 shows the *intensity dip signal* recorded by ramping the piezo voltage. This measurement indicates that there are always at least two resonances (dips) accessible within the travel range of the piezoelectric actuator. When the piezo goes out of range it is automatically reset onto the next resonance. This is shown in Figure 7 where the temperature of the OPO was monitored with a temperature sensor, whilst an identical sensor monitored the surrounding air. The change in temperature changes the cavity length and shifts the intensity dips. When the resonance dip goes out of range of the piezo it jumps to the next resonance.

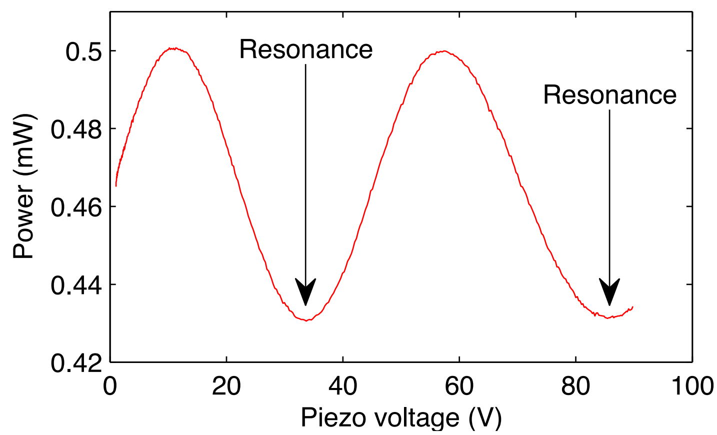


Figure 6: the intensity dip signal was measured by scanning the voltage on the piezoelectric actuator (piezo) whilst the cavity output (continuous wave) was recorded on a photodiode. The scan demonstrates that there are always two resonances within the range of travel of the piezo (a few µm).

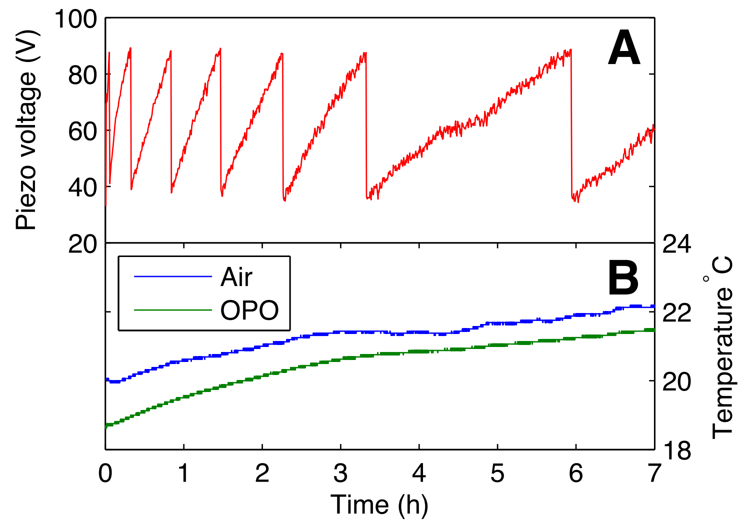


Figure 7: The stability of the cavity of the optical parametric oscillator (OPO) was monitored over the course of a day. The voltage on the piezoelectric actuator (piezo) is adjusted by a feedback loop to maintain the cavity locked on resonance at the wavelength of an injected seeded continuous wave laser (**A**). At the same time, the temperature of the OPO and the surrounding air was monitored (**B**). As the temperature gradually increases the piezo voltage approaches its limit of 100 V, and resets to a lower voltage, thus locking onto the next cavity resonance.

## 4. CONCLUSION

We have developed a custom-built laser source for differential absorption lidar and integrated it with a commercial telescope to enable measurements of atmospheric carbon dioxide. An additional wavelength reference for methane has been developed at a similar wavelength. The components of the system have been tested and are currently being integrated to create a field-ready instrument.

## ACKNOWLEDGMENTS

This work was funded by the Science and Technology Facilities Council under the Challenge-Led Applied Systems Programme and by the Natural Environment Research Council. The measurement in Figure 5D was made by Daniel Budinov.

## REFERENCES


[1] Measures, R., [Laser Remote Sensing: Fundamentals and Applications], Krieger Publishing Company, Malabar (1992).

[2] Collis, R. T. H. and Russell, P. B., "Lidar measurement of particles and gases by elastic backscattering and differential absorption" in Hinkley, E. D. (ed.), [Laser Monitoring of the Atmosphere], Springer-Verlag, Berlin & Heidelberg (1976).

[3] Robinson, R. A., Gardiner, T. D., Innocenti, F., Finlayson, A., Woods, P. T. and Few, J. F. M., "First measurements of a carbon dioxide plume from an industrial source using a ground based mobile differential absorption lidar," Env. Sci. Process. Impact 16, 1957–1966 (2014).

[4] Johnson, W., Repasky, K. S. and Carlsten, J. L., "Micropulse differential absorption lidar for identification of carbon sequestration site leakage," Appl. Opt. 52(13), 2994–3003 (2013).

[5] Mayor, S. and Spuler, S. M. "Raman-shifted eye-safe aerosol lidar," Appl. Opt. 43(19), 3915–3924 (2004).

[6] Sakaizawa, D., Nagasawa, C., Nagai, T., Abo, M., Shibata, Y., Nakazato, M. and Sakai, T., "Development of a 1.6 μm differential absorption lidar with a quasi-phase-matching optical parametric oscillator and photon-counting detector for the vertical $CO_2$ profile," Appl. Opt. 48(4), 748–757 (2009).

[7] Gibert, F., Flamant, P., Bruneau, D. and Loth, C. "Two-micrometer heterodyne differential absorption lidar measurements of the atmospheric $CO_2$ mixing ratio in the boundary layer," Appl. Opt. 45(18), 4448–4458 (2006).

[8] Refaat, T. F., Ismail, S., Koch, G. J., Rubio, M., Mack, T. L., Notari, A., Collins, J. E., Lewis, J., De Young, R., Choi, Y., Abedin, M. N. and Singh, U. N., "Backscatter 2-μm lidar validation for atmospheric $CO_2$ differential absorption lidar applications," IEEE Transactions on Geoscience and Remote Sensing 49(1), 572–580 (2010).

[9] Refaat, T. F., Ismail, S., Nehrir, A. R., Hair, J. W., Crawford, J. H., Leifer, I. and Shuman, T., "Performance evaluation of a 1.6-μm methane DIAL system from ground, aircraft and UAV platforms," Opt. Express 21(25), 30415–30432 (2013).

[10] Tang, Y., Rae, C. F., Rahlff, C. and Dunn, M. H., "Low-threshold, high-efficiency, widely tunable infrared source from a KTP-based optical parametric oscillator," J. Opt. Soc. Am. B 14(12), 3442–3451 (1997).

[11] Li, S. G., Li, H. H., Ma, X. H., Wang, J. T., Zhu, X. L. and Chen, W. B., "High-efficiency nanosecond optical parametric oscillator with the stable ring configuration," Laser Phys. 22(10), 1610–1614 (2012).

[12] He, Y., Baxter, G. W., and Orr, B. J., "Locking the cavity of a pulsed periodically poled lithium niobate optical parametric oscillator to the wavelength of a continuous-wave injection seeder by an "intensity-dip" method," Rev. Sci. Instrum. 70(8), 3203 (1999).

[13] Amediek, A., Fix, A., Wirth, M. and Ehret, G., "Development of an OPO system at 1.57 μm for integrated path DIAL measurement of atmospheric carbon dioxide," Appl. Phys. B 92(2), 295–302 (2008).

[14] Rothman, L. S., et al., "The HITRAN2012 molecular spectroscopic database," *J. Quant. Spectrosc. Radiat. Transf.* 130, 4–50 (2013).